Chemistry–A European Journal
Research Article
doi.org/10.1002/chem.202200326
Chemistry Europe
European Chemical Societies Publishing
www.chemeurj.org

Fully Bridged Triphenylamines Comprising Five- and Seven-Membered Rings

Ina Michalsky,[a, b] Viktoria Gensch,[c] Christian Walla,[d] Marvin Hoffmann,[d] Frank Rominger,[a] Thomas Oeser,[a] Petra Tegeder,[e] Andreas Dreuw,[d] and Milan Kivala*[a, b]

Abstract: A family of fully bridged triphenylamines with embedded 5- and 7-membered rings is presented. The compounds are potent electron donors capable to undergo donor/acceptor interactions with strong cyano-based acceptors both in the solid state and solution. These interactions were evaluated by IR and UV/vis spectroscopy as well as X-ray crystallography. The vinylene-bridged compound was oxidized to the corresponding 1,2-diketone which readily underwent acid-catalyzed condensation with selected 1,2-phenylenediamines. The resulting π-extended quinoxaline derivatives represent valuable building blocks for the development of functional chromophores upon appropriate functionalization.

Introduction

Triphenylamine (TPA) is widely applied as a structural element in hole-transporting materials and donor–acceptor systems, on account of its good electron donating properties.[1] TPAs were successfully implemented into charge-transfer complexes[2] with appealing materials characteristics.[3] Even though a negative inductive effect is exerted from the central nitrogen atom, withdrawing electron density from the adjacent aromatic moieties, this effect is outweighed by its mesomeric contribution. Thereby the nitrogen atom with its lone pair of electrons supplies the aromatic rings and facilitates oxidation, supported by delocalization of the resulting positive charge throughout the adjacent phenyls.[4] However, TPA has a propeller-shaped geometry, which considerably reduces the efficient electronic communication.[5] Hence, planarization of TPA by suitable bridging moieties is a potent approach to enhance π-conjugation and thus the respective electron donating properties.[6] In this context, the smallest bridged TPA is the doubly pentagon-fused TPA **1** (Scheme 1), which was first synthesized by *Dunlop* and *Tucker* already back in 1939.[7] Other bridging units include carbonyl or dimethylmethylene bridges, which can be found in the *N*-heterotriangulenes (*N*-HTAs) realized by *Hellwinkel* and *Melan* in the 1970s.[8] Recently, doubly carbonyl-bridged HTAs with an additional oxygen, sulfur, or dimethylmethylene bridge were reported by *Jiang, Liao* and coworkers.[9] Of course, bridged TPAs are not limited to *N*-HTAs comprising exclusively 6-membered rings.[10] For exam-

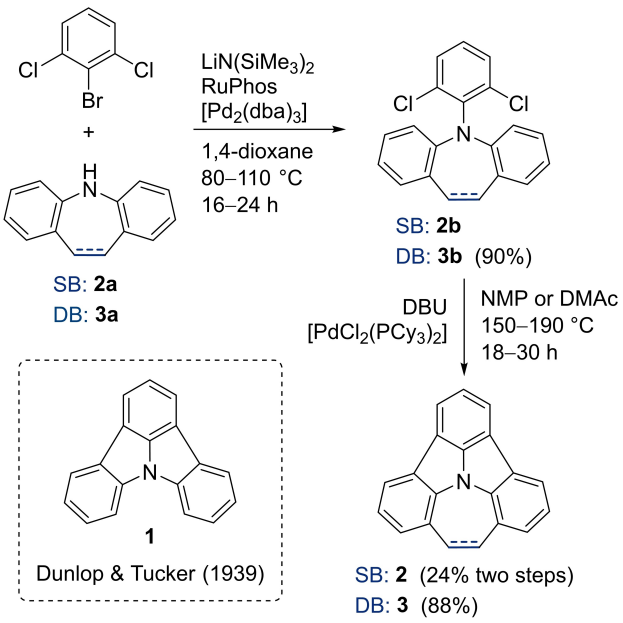

Scheme 1. Known doubly bridged TPA **1**.[7] Synthesis of fully bridged TPAs **2** and **3**. SB = single bond, DB = double bond.

[a] *I. Michalsky, Dr. F. Rominger, Dr. T. Oeser, Prof. Dr. M. Kivala*
Organisch-Chemisches Institut, Universität Heidelberg
Im Neuenheimer Feld 270, 69120 Heidelberg (Germany)
E-mail: milan.kivala@oci.uni-heidelberg.de

[b] *I. Michalsky, Prof. Dr. M. Kivala*
Centre for Advanced Materials, Universität Heidelberg
Im Neuenheimer Feld 225, 69120 Heidelberg (Germany)

[c] *Dr. V. Gensch*
Department Chemie und Pharmazie, Universität Erlangen-Nürnberg
Nikolaus-Fiebiger-Strasse 10, 91058 Erlangen (Germany)

[d] *C. Walla, Dr. M. Hoffmann, Prof. Dr. A. Dreuw*
Interdisziplinäres Zentrum für Wissenschaftliches Rechnen, Universität Heidelberg
Im Neuenheimer Feld 205 A, 69120 Heidelberg (Germany)

[e] *Prof. Dr. P. Tegeder*
Physikalisch-Chemisches Institut, Universität Heidelberg
Im Neuenheimer Feld 253, 69120 Heidelberg (Germany)

Supporting information for this article is available on the WWW under https://doi.org/10.1002/chem.202200326

ple, the incorporation of two 5-membered rings results in a pronounced steric strain and consequently the doubly pentagon-fused TPA with an additional methylene or carbonyl bridge possesses a curved structure.[10c,e] In spite of these appealing achievements, the structural diversity of bridged TPAs still remains rather narrow, which motivated us to explore the introduction of extended bridging moieties comprising two carbon atoms.

Herein, we present the synthesis and properties of a family of fully bridged TPAs incorporating a 7-membered ring on account of ethylene or vinylene bridging units. The rigid vinylene bridge not only enforces the planarity of the polycyclic scaffold but also provides for further derivatization and π-expansion. Furthermore, the vinylene-bridged compound co-crystallizes with several paradigmatic cyano-based electron acceptors.

Results and Discussion

To obtain a comparable series of differently bridged TPAs, compound **1** was synthesized according to a modified procedure starting from 9*H*-carbazole (for synthetic details, see the Supporting Information).[11] Both novel compounds **2** and **3** were obtained by *Buchwald-Hartwig* coupling, followed by Pd-mediated cyclization as the key steps (Scheme 1).

Iminodibenzyl **2a** was *N*-arylated[12] with 2-bromo-1,3-dichlorobenzene in the presence of $LiN(SiMe_3)_2$, {2′,6′-bis[(propan-2-yl)oxy][1,1′-biphenyl]-2-yl}(dicyclohexyl)phosphane (RuPhos), and tris(dibenzylideneacetone)dipalladium(0) to deliver compound **2b** in 18% yield after purification. However, for subsequent cyclization precursor **2b** was used without further purification, which surprisingly delivered better results. Iminostilbene **3a** was *N*-arylated under analogous conditions to afford compound **3b** in 90% yield after purification. Final Pd-mediated cyclization of **2b** and **3b** was performed using dichlorobis(tricyclohexylphosphine)palladium(II) under basic conditions at elevated temperature to deliver target compounds **2** (24% overall yield) and **3** (88% yield) as colorless and orange solid, respectively.

Single crystals of **2** and **3** were grown by diffusing petroleum ether or hexanes into a solution of the respective compound in dichloromethane at room temperature (Figure 1a,b). The nitrogen center in **2** with its relatively flexible ethylene bridge is slightly pyramidalized as expressed by the sum of the C–N–C bond angles $\Sigma\sphericalangle_{C-N-C}$ amounting to 357.9° (average over both independent molecules). Consequently, the 7-membered ring is slightly tilted. In contrast, compound **3** possesses a virtually planar conformation with $\Sigma\sphericalangle_{C-N-C}$ of 359.9° as a result of the rigid vinylene bridge. The bond lengths of the C–C and C=C moieties within the 7-membered rings of **2** and **3**, respectively, are slightly elongated compared to those reported for parent iminodibenzyl (1.52 Å) and iminostilbene (1.32°Å).[13] However, the common single and double bond character of these moieties is further corroborated by the corresponding ^{1}H NMR signals occurring at 3.52 and 5.89 ppm for **2** and **3**, respectively (see the Supporting Information).

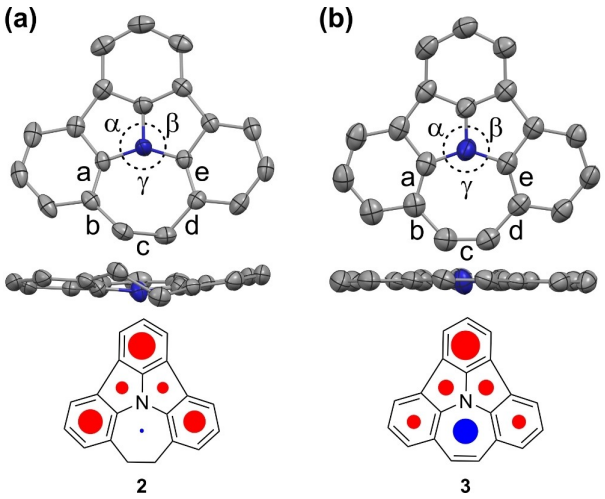

Figure 1. X-ray crystal structures and nucleus-independent chemical shifts (NICS(1)) of **2** and **3** (50% probability level, H-atoms omitted). Color code: grey = carbon, blue = nitrogen. (a) Selected bond lengths of **2** (two independent molecules in the unit cell) [Å] c = 1.552(4)/1.556(4); bond angles [°] α = 108.9(2)/108.7(2); β = 108.5(2)/108.1(2); γ = 140.5(2)/141.0(2). Rounded torsion angles a-b-c 40°/40° and e-d-c 51°/53°. (b) Selected bond lengths of **3** [Å] c = 1.362(3); bond angles [°] α = 109.11(18); β = 108.92(19); γ = 141.9(2); rounded torsion angles a-b-c 2° and e-d-c 2°. Relative aromaticity (red) and antiaromaticity (blue) of **2** and **3** is schematically displayed by the size of the solid dots.

To obtain information about the local aromaticity and antiaromaticity within the polycyclic frameworks of **2** and **3**, nucleus independent chemical shifts NICS(1) were calculated using DFT at the B3LYP–D/6-31G* level of theory (Figure 1a,b).[14] Our results suggest a considerable aromatic character for all 5- and 6-membered rings in both compounds. At the same time, the calculated NICS values point towards certain antiaromaticity of both 7-membered moieties. While in compound **2** with its saturated ethylene bridge the calculated positive NICS value appears meaningless, the cycloheptatriene ring in **3** displays a pronounced antiaromatic character.

Parent TPA possesses one absorption band in the UV region between 250 and 350 nm.[15] In comparison, compound **1** displays several absorption maxima, whereby the lowest energy maximum λ_{max} is located at 363 nm (Figure 2, Table 1). A broad absorption band between 368 and 376 nm without a defined maximum is observed for compound **2** featuring the saturated ethylene bridge. Compound **3** with the vinylene bridge shows a very broad absorption band with an apparent fine structure in the low energy region reaching to 500 nm. While the high energy absorptions most likely originate from π–π* and n–π* transitions, the longer wavelength bands may be attributable to HOMO–LUMO transitions.[9,15]

The progressive red-shift of λ_{max} within the series of compounds **1**, **2** and **3** can be most likely ascribed to improved overall π-conjugation due to the unsaturated vinylene bridge. The optical bandgap E_g^{opt} extracted from the absorption edge wavelength λ_{ae} indicates continuous narrowing from 3.30 eV for

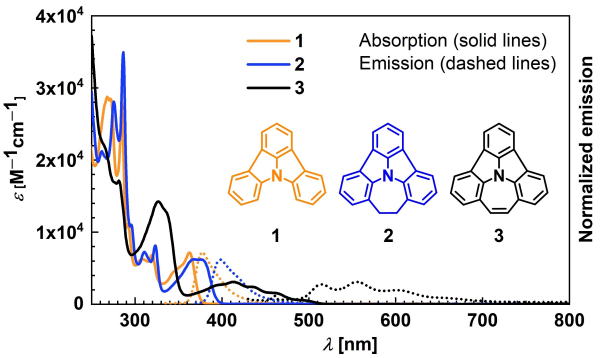

Figure 2. UV/vis spectra of compounds **1**, **2**, and **3** recorded in CH_2Cl_2 at room temperature.

Table 2. Selected structural and spectroscopic data of the donor/acceptor systems involving **3**.

Acceptor	$\Sigma\measuredangle_{C\text{–}N\text{–}C}$[a] [°]	$\tilde{\nu}_{C\equiv N}$[b] [cm^{-1}]	λ_{max}[c] [nm]
TCNE	360.0	2251, 2221 (2258, 2221)	730
TCNQ	358.7/356.6	2220 (2224)	885
F_4TCNQ	358.3	2219 (2226)	1190

[a] Average values for all independent molecules of **3** in the respective unit cell. [b] Recorded in the solid state using the co-crystal (TCNE, TCNQ) or the amorphous solid obtained upon evaporation of the 1:1 donor/acceptor mixture in CH_2Cl_2 (F_4TCNQ) by FTIR (ATR). Values in parentheses correspond to pristine acceptor. [c] Recorded in CH_2Cl_2 at rt. λ_{max} denotes maximum absorption wavelength.

the doubly pentagon-fused **1** to 2.39 eV corresponding to vinylene-bridged **3**. For comparison, parent TPA features a considerably larger E_g^{opt} of 3.65 eV.[15] Compounds **1**–**3** exhibit fluorescence in CH_2Cl_2. While **1**[16] and **2** possess moderate photoluminescence quantum yields (PLQYs) of 0.16, the value for vinylene-bridged **3** is below 0.02 (Table S14 in the Supporting Information).

Cyclic voltammetry was employed to investigate the electrochemical behavior of the compounds in CH_2Cl_2 with a scan rate of 50 mV sec^{-1} (for details, see the Supporting Information). Compound **2** exhibits an irreversible oxidation with a peak potential of +1.01 V (vs. ferrocene/ferrocenium (Fc/Fc^+)) in the anodic trace, and a corresponding peak potential of +0.67 V in the cathodic trace (Figure S41). Additional oxidation events are observed for compounds **2** and **3**, for example at +0.30 V and +0.82 V in the cathodic trace, respectively, which most likely originate from the products formed by follow-up reactions of the initially formed radical cation in analogy to unsubstituted TPA.[17] For compound **3**, the first oxidation process can be ascribed as quasi-reversible (Figure S42). Hereby, the peak potential for the first oxidation is found at +0.66 V and the corresponding peak potential with the lowest positive voltage in the cathodic trace occurs at +0.53 V. In comparison, **3** is more easily oxidized than the corresponding derivative with the saturated ethylene bridge **2**, which has, in turn, a lower first oxidation peak potential than the doubly pentagon-fused **1**.[18]

This trend is in good agreement with the DFT calculated vertical and adiabatic ionization potentials reaching the lowest values of 6.51 and 6.42 eV, respectively, for compound **3** with the π-conjugated vinylene bridge (for the complete data set including the calculated HOMO and LUMO energies, see Table 1 and the Supporting Information). These data identify compound **3** as the most potent electron donor of the series for which reason its ability to undergo donor/acceptor interactions with tetracyanoethylene (TCNE; $E_{red,1} = -0.32$ V vs. Fc/Fc^+ in CH_2Cl_2), 7,7,8,8-tetracyanoquinodimethane (TCNQ; $E_{red,1} = -0.25$ V), and 2,3,5,6-tetrafluoro-7,7,8,8-tetracyanoquinodimethane (F_4TCNQ; $E_{red,1} = +0.16$ V) as paradigmatic electron acceptors was investigated.[19] To evaluate the interactions X-ray crystallography, UV/vis absorption, and IR spectroscopy were used.

Co-crystals of **3** with the particular acceptor were grown by liquid diffusion of petroleum ether into a solution of both components (1:1) in CH_2Cl_2 at room temperature. Alternating, slightly inclined 1:1 stacks are formed with TCNE in which the donor retains its planarity with the C–N–C bond angles summing up to 360° (Figure 3a). Moreover, basically no bond length deviations of the C=C bond (1.349(2) Å) and the average C–CN bond (1.440(3) Å) of co-crystallized TCNE are observed with respect to pristine TCNE (C=C 1.349(6) Å and C–CN 1.435(4) Å).[20] This finding points towards weak charge transfer between **3** and TCNE in the solid state.[20,21] The asymmetric unit of **3** co-crystallized with the stronger acceptor TCNQ consists of one donor molecule stacked in an alternate fashion with the acceptor in a distance ranging from 3.29 Å to 3.34 Å (Figure 3b, Table 2).

Interestingly, in this case the donor molecules are slightly curved with the nitrogen centers showing weak pyramidalization. At the same time, the donor molecules are rotated and

Table 1. Experimental and theoretical optoelectronic data of the title compounds.

	λ_{max} [nm][a]	ε [M^{-1} cm^{-1}][a]	λ_{em} [nm][a]	λ_{ae} [nm]	E_g^{opt} [eV][b]	EA_v /EA_a [eV][c]	IP_v /IP_a [eV][c]	HOMO/LUMO [eV][d]
1	363	7200	378	376	3.30	−0.22/−0.12	7.06/7.00	−5.55/−1.25
2	368–376	6200	398	395	3.14	−0.25/−0.12	6.82/6.77	−5.36/−1.20
3	414	3100	514, 556, 602	518	2.39	0.25/0.37	6.51/6.42	−5.03/−1.71

[a] Recorded in CH_2Cl_2; λ_{max} denotes maximum absorption wavelength; ε denotes molar absorption coefficient. [b] Optical band gaps calculated according to $E_g^{opt} = h \times c/\lambda_{ae}$. The absorption edge wavelength λ_{ae} was determined with a tangent at the longest-wavelength absorption maximum λ_{max}, h denotes the *Planck* constant and c the speed of light. [c] Vertical and adiabatic electron affinity (EA_v and EA_a) and ionization potential (IP_v and IP_a) calculated at the B3LYP–D/6-31G* level of theory as difference of the total energies of the cation/anion and the neutral species. [d] Calculated at the B3LYP/6-31G*.

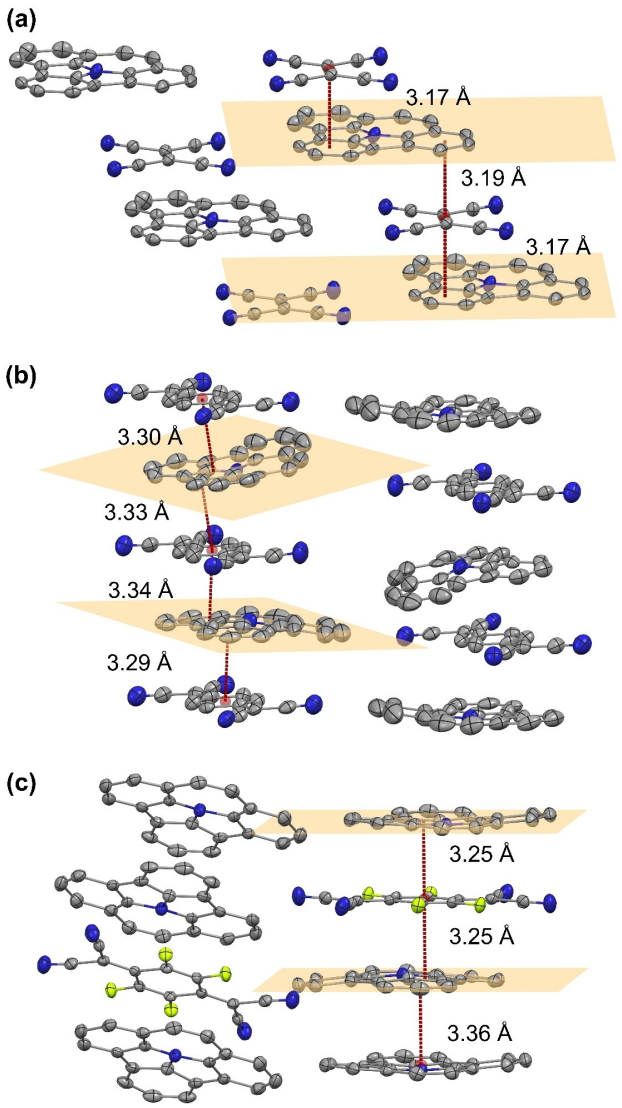

Figure 3. X-ray crystal structures of **3** with electron acceptors **TCNE** (a), **TCNQ** (b), and **F_4TCNQ** (c) with selected distances (50% probability level, H-atoms and solvent molecules omitted). Color code: grey = carbon, blue = nitrogen, green = fluorine, orange = plane through all non-H-atoms of **3**, red dot = centroid through all atoms of respective molecule except H-atoms.

not parallel with respect to each other. The average lengths of the exocyclic C=C (1.383(11) Å) and C≡N bonds (1.153(10) Å) of co-crystallized TCNQ are identical to those of pristine TCNQ.[22] F_4TCNQ, as the strongest acceptor of the series, co-crystalizes with **3** in columns with a stoichiometric ratio of 1:2 (Figure 3c). The distance between **3** and the acceptor within the column is 3.25 Å and the respective columns are slightly inclined with respect to each other. Also in this case the donor molecule is slightly curved with the nitrogen atom pointing towards the acceptor. However, the structural features of F_4TCNQ remain unaffected upon co-crystallization.[23]

Further insights into the interactions between **3** and the particular acceptor were obtained by IR spectroscopy. Although no significant changes of the C≡N bond lengths in the co-crystals were discernible by X-ray crystallography, a shift of the C≡N stretching frequency towards lower wavenumbers with respect to the pristine acceptors is observed in all cases (Table 2). The weakening of the C≡N bonds suggests a certain degree of charge transfer between **3** and the acceptor in the solid state.[24] This is further supported by the occurrence of the characteristic strongly bathochromically shifted broad absorption bands in the UV/vis spectra of the concentrated solutions of **3** and the acceptor in THF (TCNE) or 1,2-dichloroethane (TCNQ, F_4TCNQ; see the Supporting Information).

The 7-membered ring in **3** with its olefinic C=C bond provides for further functionalization towards π-extended derivatives. To demonstrate the versatility of this approach, compound **3** was successfully oxidized with SeO_2 in *o*-dichlorobenzene (*o*-DCB) at 200 °C towards diketone **4** (Figure 4a). Subsequent condensation reactions of **4** with suitable 1,2-phenylenediamines under acidic conditions delivered unprecedented quinoxalines **5** and **6** in good yields. The compounds are yellow to red solids which are sparingly soluble in common chlorinated solvents. The longest wavelength UV/vis absorptions of **5** and **6** occur in CH_2Cl_2 at 427 nm and 483 nm, respectively. Both compounds **5** and **6** are fluorescent in solution with the maximum emission at 500 nm and 559 nm and PLQYs of 0.36 and 0.61, respectively. X-ray crystallographic analysis unambiguously confirmed the structural identity of

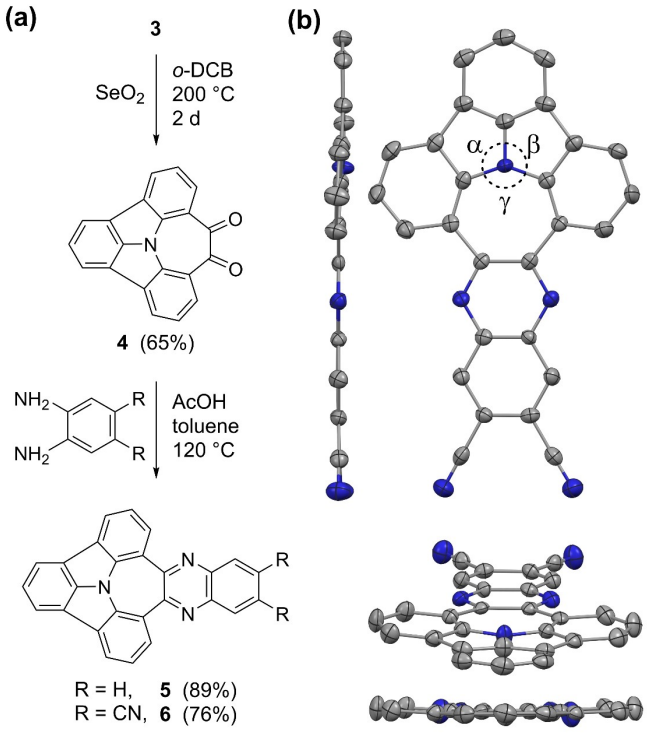

Figure 4. (a) Further transformations of **3** towards quinoxalines **5** and **6**. (b) X-ray crystal structure at 50% probability ellipsoids of **6** with $P2_1/c$ space group. Hydrogen atoms and solvent molecules are omitted for clarity. Color code: grey = carbon, blue = nitrogen. Selected binding angles [°] α = 109.6(4); β = 108.8(4); γ = 141.3(4). From upper left to lower right: side view, top view, two front views at different viewing angles.

both quinoxalines (Figure 4b and the Supporting Information). For example, compound **6** crystallizes in two polymorphic forms with a perfectly planar polycyclic framework. In all cases, the nitrogen centers display basically no pyramidalization. The electron-deficient pyrazine ring in combination with the cyano substituents considerably increase the calculated electron affinity of **6** (EA_v/EA_a 1.67/1.80 eV vs. 0.25/0.37 eV (for parent **3**)). The electron accepting properties of **6** are documented by the two quasi-reversible reduction events observed by cyclic voltammetry in CH_2Cl_2 with the first reduction occurring at a peak potential of -1.64 V (vs. Fc/Fc^+ in 1,2-dichlorobenzene; see Figure S45 in the Supporting Information).

Conclusion

In summary, we established a reliable synthetic route to a new family of fully bridged TPAs with embedded 5- and 7-membered rings. The compounds behave as potent electron donors capable to undergo donor/acceptor interactions with cyano-based acceptors both in the solid state and solution. The interactions were evaluated by IR and UV/vis spectroscopy as well as X-ray crystallography. The synthetic versatility of the vinylene-bridged compound was demonstrated by oxidation to the corresponding 1,2-diketone followed by condensation with selected 1,2-phenylenediamines. The resulting electron-deficient polycycles represent valuable building blocks for the development of functional chromophores upon appropriate functionalization.

Experimental Section

Experimental details and characterization data can be found in the Supporting Information. Deposition Numbers (**S1**, for structure see the Supporting Information), 2145720 (**1**), 2145721 (**2b**), 2145722 (**2**), 2145723 (**3b**), 2145724 (**3**), 2145725 (**4**), 2145726 (**3** with TCNE), 2145727 (**3** with TCNQ), 2145728 (**3** with F_4TCNQ), 2145729 (**5**), 2145730 (**6**, polymorph I), and 2145731 (**6**, polymorph II) contain(s) the supplementary crystallographic data for this paper. These data are provided free of charge by the joint Cambridge Crystallographic Data Centre and Fachinformationszentrum Karlsruhe Access Structures service.

Acknowledgements

Generous funding by the Deutsche Forschungsgemeinschaft (DFG) – Project number 281029004-SFB 1249 (Projects A05, B01, B06) and project number 401247651-KI 1662/3-1 is gratefully acknowledged. Open Access funding enabled and organized by Projekt DEAL.

Conflict of Interest

The authors declare no conflict of interest.

Data Availability Statement

The data that support the findings of this study are available from the corresponding author upon reasonable request.

Keywords: bridged triarylamines · charge transfer · co-crystallization · electron donor · N-heterocycle

[1] a) P. Agarwala, D. Kabra, *J. Mater. Chem. A* **2017**, *5*, 1348–1373; b) A. Iwan, D. Sek, *Prog. Polym. Sci.* **2011**, *36*, 1277–1325; c) S. Jhulki, J. N. Moorthy, *J. Mater. Chem. C* **2018**, *6*, 8280–8325; d) S. Shahnawaz, S. Sudheendran Swayamprabha, M. R. Nagar, R. A. K. Yadav, S. Gull, D. K. Dubey, J.-H. Jou, *J. Mater. Chem. C* **2019**, *7*, 7144–7158; e) Y. Tao, C. Yang, J. Qin, *Chem. Soc. Rev.* **2011**, *40*, 2943–2970; f) J. Urieta-Mora, I. García-Benito, A. Molina-Ontoria, N. Martín, *Chem. Soc. Rev.* **2018**, *47*, 8541–8571.
[2] a) J. Zhang, W. Xu, P. Sheng, G. Zhao, D. Zhu, *Acc. Chem. Res.* **2017**, *50*, 1654–1662; b) W. Wang, L. Luo, P. Sheng, J. Zhang, Q. Zhang, *Chem. Eur. J.* **2021**, *27*, 464–490.
[3] a) Z. Wang, F. Yu, J. Xie, J. Zhao, Y. Zou, Z. Wang, Q. Zhang, *Chem. Eur. J.* **2020**, *26*, 3578–3585; b) J. Han, W. Feng, D. Y. Muleta, C. N. Bridgmohan, Y. Dang, G. Xie, H. Zhang, X. Zhou, W. Li, L. Wang, D. Liu, Y. Dang, T. Wang, W. Hu, *Adv. Funct. Mater.* **2019**, *29*, 1902503; c) S. Wang, W. Sun, M. Zhang, H. Yan, G. Hua, Z. Li, R. He, W. Zeng, Z. Lan, J. Wu, *RSC Adv.* **2020**, *10*, 38736–38745.
[4] X. Zhao, M. Wang, *Mater. Today Energy* **2018**, *7*, 208–220.
[5] A. N. Sobolev, V. K. Belsky, I. P. Romm, N. Y. Chernikova, E. N. Guryanova, *Acta Crystallogr. Sect. C* **1985**, *41*, 967–971.
[6] a) N. Hammer, T. A. Schaub, U. Meinhardt, M. Kivala, *Chem. Rec.* **2015**, *15*, 1119–1131; b) M. Hirai, N. Tanaka, M. Sakai, S. Yamaguchi, *Chem. Rev.* **2019**, *119*, 8291–8331; c) T. A. Schaub, K. Padberg, M. Kivala, *J. Phys. Org. Chem.* **2020**, *33*, e4022.
[7] H. G. Dunlop, S. H. Tucker, *J. Chem. Soc.* **1939**, 1945–1956.
[8] a) D. Hellwinkel, M. Melan, *Chem. Ber.* **1971**, *104*, 1001–1016; b) D. Hellwinkel, M. Melan, *Chem. Ber.* **1974**, *107*, 616–626.
[9] S.-N. Zou, C.-C. Peng, S.-Y. Yang, Y.-K. Qu, Y.-J. Yu, X. Chen, Z.-Q. Jiang, L.-S. Liao, *Org. Lett.* **2021**, *23*, 958–962.
[10] a) D. Hellwinkel, W. Schmidt, *Chem. Ber.* **1980**, *113*, 358–384; b) M. Ito, R. Kawasaki, K. S. Kanyiva, T. Shibata, *Eur. J. Org. Chem.* **2016**, 5234–5237; c) N. Deng, G. Zhang, *Org. Lett.* **2019**, *21*, 5248–5251; d) Y. Zagranyarski, A. Skabeev, Y. Ma, K. Müllen, C. Li, *Org. Chem. Front.* **2016**, *3*, 1520–1523; e) L. Zhou, G. Zhang, *Angew. Chem. Int. Ed.* **2020**, *59*, 8963–8968; *Angew. Chem.* **2020**, *132*, 9048.
[11] P. Kautny, D. Lumpi, Y. Wang, A. Tissot, J. Bintinger, E. Horkel, B. Stöger, C. Hametner, H. Hagemann, D. Ma, J. Fröhlich, *J. Mater. Chem. C* **2014**, *2*, 2069–2081.
[12] W. Huang, S. L. Buchwald, *Chem. Eur. J.* **2016**, *22*, 14186–14189.
[13] a) J. P. Reboul, B. Cristau, J. Estienne, J. P. Astier, *Acta Crystallogr. Sect. B* **1980**, *36*, 2108–2112; b) J. P. Reboul, B. Cristau, J. C. Soyfer, J. Estienne, *Acta Crystallogr. Sect. B* **1980**, *36*, 2683–2688.
[14] a) Z. Chen, C. S. Wannere, C. Corminboeuf, R. Puchta, P. v. Ragué Schleyer, H. Jiao, N. J. R. v. Eikema Hommes, V. G. Malkin, O. L. Malkina, *J. Am. Chem. Soc.* **1997**, *119*, 12669–12670; Schleyer, *Chem. Rev.* **2005**, *105*, 3842–3888; Schleyer, *Chem. Rev.* **2005**, *105*, 3842–3888; b) P. v. Raagué Schleyer, H. Jiao, N. J. R. v. Eikema Hommes, V. G. Malkin, O. L. Malkina, *J. Am. Chem. Soc.* **1997**, *119*, 12669–12670; c) P. v. R. Schleyer, C. Maerker, A. Dransfeld, H. Jiao, N. J. R. v. Eikema Hommes, *J. Am. Chem. Soc.* **1996**, *118*, 6317–6318.
[15] Z. Fang, V. Chellappan, R. D. Webster, L. Ke, T. Zhang, B. Liu, Y.-H. Lai, *J. Mater. Chem.* **2012**, *22*, 15397–15404.
[16] S. I. Wharton, J. B. Henry, H. McNab, A. R. Mount, *Chem. Eur. J.* **2009**, *15*, 5482–5490.
[17] a) R. F. Nelson, R. N. Adams, *J. Am. Chem. Soc.* **1968**, *90*, 3925–3930; b) E. T. Seo, R. F. Nelson, J. M. Fritsch, L. S. Marcoux, D. W. Leedy, R. N. Adams, *J. Am. Chem. Soc.* **1966**, *88*, 3498–3503; c) K. Sreenath, C. V. Suneesh, V. K. R. Kumar, K. R. Gopidas, *J. Org. Chem.* **2008**, *73*, 3245–3251; d) X. Zheng, X. Wang, Y. Qiu, Y. Li, C. Zhou, Y. Sui, Y. Li, J. Ma, X. Wang, *J. Am. Chem. Soc.* **2013**, *135*, 14912–14915.
[18] J. B. Henry, S. I. Wharton, E. R. Wood, H. McNab, A. R. Mount, *J. Phys. Chem. A* **2011**, *115*, 5435–5442.

[19] M. Kivala, C. Boudon, J.-P. Gisselbrecht, B. Enko, P. Seiler, I. B. Müller, N. Langer, P. D. Jarowski, G. Gescheidt, F. Diederich, *Chem. Eur. J.* **2009**, *15*, 4111–4123.
[20] J. S. Miller, *Angew. Chem. Int. Ed.* **2006**, *45*, 2508–2525; *Angew. Chem.* **2006**, *118*, 2570–2588.
[21] a) P. Becker, P. Coppens, F. K. Ross, *J. Am. Chem. Soc.* **1973**, *95*, 7604–7609; b) R. G. Little, D. Pautler, P. Coppens, *Acta Crystallogr. Sect. B* **1971**, *27*, 1493–1499.
[22] R. E. Long, R. A. Sparks, K. N. Trueblood, *Acta Crystallogr.* **1965**, *18*, 932–939.
[23] N. T. Johnson, M. R. Probert, P. G. Waddell, *Acta Crystallogr. Sect. C* **2021**, *77*, 426–434.
[24] K. P. Goetz, D. Vermeulen, M. E. Payne, C. Kloc, L. E. McNeil, O. D. Jurchescu, *J. Mater. Chem. C* **2014**, *2*, 3065–3076.

Manuscript received: February 2, 2022
Accepted manuscript online: March 16, 2022
Version of record online: May 9, 2022